

EXPERIMENTAL INVESTIGATION OF VISCOSITY AND SPECIFIC HEAT CAPACITY OF IRON OXIDE FLUIDS FOR HEAT TRANSFER APPLICATIONS

Dalibor NOVÁK, Lenka ŘEHÁČKOVÁ, Vlastimil NOVÁK, Silvie ROSYPALOVÁ,
Dalibor MATÝSEK, Monika KAWULOKOVÁ, Simona ZLÁ, Aneta SMÝKALOVÁ,
Bedřich SMETANA, Lubomíra DROZDOVÁ

VSB - Technical University of Ostrava, Ostrava, Czech Republic, EU,

dalibor.novak.st1@vsb.cz, lenka.rehackova@vsb.cz, vlastimil.novak@vsb.cz, silvie.rosypalova@vsb.cz,
dalibor.matysek@vsb.cz, monika.kawulokova@vsb.cz, simona.zla@vsb.cz, aneta.smykalova@vsb.cz,
bedrich.smetana@vsb.cz, lubomira.drozdoва@vsb.cz

<https://doi.org/10.37904/metal.2022.4453>

Abstract

Modifying liquids with nanoparticles is widely recognized as a practical approach for improving their heat transfer characteristics without significantly increasing viscosity. This work examines the effect of adding hematite and acid-leached blast furnace sludge particles on the rheological and thermal properties of deionized water. The investigated fluids were prepared by dispersing a certain amount of hematite and leached blast furnace sludge particles in distilled water using a sonicator. The modifier content in the liquid varied up to 5 wt%. Pristine iron oxides with particle sizes of approximately 5 micrometers and 50 nanometers were used as model systems. Leached sludge particles were deagglomerated for an extended period prior to measurement. The rheological behavior of the fluids was studied using an FRS 1600 furnace rheometer system designed for viscosity measurement from 1 mPa·s, and the specific heat capacity of hematite and leached blast furnace sludge was obtained by SENSYS EVO TG-DSC calorimeter equipped with 3D-sensor technology. Furthermore, the characterization of the prepared liquids was also supported by the results of SEM analysis. The results of this study provide the foundation for the use of leached blast furnace sludge as a potential heat transfer fluid.

Keywords: Heat transfer fluid, iron oxides, blast furnace sludge, viscosity, specific heat capacity

1. INTRODUCTION

Enhancement of heat transfer fluids (HTFs) efficiency has been a matter of ongoing research over the past decades and is currently driven primarily by the increasing worldwide demand for energy. Typically, adding micro- or nanosized particles to base fluids is a conventional route to achieve this goal. Metals and some metal oxides are considered suitable modifiers because, for instance, their thermal conductivity at room temperature is many orders of magnitude higher than that of conventional fluids. Therefore, the thermal conductivity of fluids containing suspended metallic particles is significantly larger. Until 1995, when Choi came up with the novel idea of suspending nanoparticles in common heat transfer fluids, microparticles were used for modification [1]. Suspensions containing microparticles suffered severe disadvantages, such as abrasion, sedimentation, clogging, and erosion. Nevertheless, the dispersion of nanosized particles can aggregate and form clusters due to the higher surface energy [2,3]. Still, nanoparticles significantly improve the effective thermal conductivity of the suspension as they have a large surface-to-volume ratio compared to a suspension of micrometer-sized particles [4]. It is well known that heat transfer occurs at the surface of particles, which is, of course, noticeably larger for nanoparticles, and therefore, they markedly improve the thermofluidic behavior of heat transfer fluids [1].

Knowledge of the viscosity and heat capacity of a given HTF is required for the proper performance of the thermal system. Viscosity is essential for assessing fluid resistance, and key parameters of the transfer system,

such as pumping power and pressure drop, are directly dependent on it [5]. On the other hand, viscosity is affected by many parameters, e.g., particle size and shape, temperature, volume concentration, acidity (pH value), shear rate, particle aggregation, base fluid type, and preparation method, which opens a wide field for optimization [6]. It is worth mentioning that models are derived based on the assumption of linear dependence of base fluid viscosity on volume concentration. Nevertheless, these models fail to describe the nanofluid's viscosity as a function of temperature. Therefore, to model the influence of volume concentration, temperature and particle size, ad hoc models are necessary [7,8]. The study of the specific heat capacity of heat transfer fluids has not attracted as much attention, although it is a key thermal property in energy systems. It is a property that determines nanofluid heat storage capacity and is required to calculate thermal diffusivity and dynamic thermal conductivity [9]. The heat capacity of HTFs can be either similar or different from that of the base liquid depending on the heat capacity of the modifying particles and is mainly affected by volume concentration and temperature [10].

Modification of liquid carriers by iron oxides contributes to enhancing thermal conductivity. There are many reports documenting improvements in thermal conductivity values when magnetite and hematite (nano)particles of different concentrations and sizes are added with or without an externally applied magnetic field [11-14]. These studies show that the thermal conductivity of magnetic nanofluids increases with the particle volume fraction and temperature when a magnetic field is damped. Nevertheless, there is still a scarcity of research articles about the effect of iron oxides on the heat capacity and viscosity of heat transfer fluids.

This study aims to contribute to the still growing area of research on heat transfer fluids by exploring blast furnace sludge (BFS) as a potential modifier. For this purpose, nano- and microsized particles of hematite, one of the main BFS phases, were used as model systems, and BFS was pretreated by acid leaching and long-time sonication.

2. EXPERIMENTAL RESEARCH

2.1. Preparation of heat transfer fluids

The fluids were prepared by dispersing micro and nanoparticles of hematite in deionized water, and the mass concentrations of the prepared suspensions were 1, 3, and 5 wt%. The average sizes of the microhematite and nanohematite particles were 5 μm and 50 nm, respectively. Subsequently, hematite samples were exposed to ultrasound (Elmasonic S15H) for 1 hour. The blast furnace sludge, purchased from Liberty Ostrava a.s., was pretreated by grinding, sieving (below 0.18 mm) and leaching for 48 h in 1 M HCl to remove calcium, zinc, magnesium, and other metals and elements, leaving the metal oxide content almost unchanged (**Table 1**). X-ray diffraction analysis of leached blast furnace sludge revealed that the main phases are hematite and magnetite (**Table 2**).

Table 1 Composition of unleached and leached sludge

Component	unleached (wt%)	leached (wt%)
Fe total	39.00	47.00
FeO	5.78	4.64
Mg	0.97	0.35
Al	1.27	0.96
S	0.53	0.37
K	0.14	0.12
Ca	6.34	0.27
Cr	0.03	0.03
Mn	0.27	0.09
Zn	0.67	0.05

Table 2 Crystalline phases of leached sludge

Phase	(wt%)
Amorphous content	48.76
Hematite	33.01
Magnetite	11.47
Quartz	6.17
Cristobalite	0.59

2.2. Measurement of rheological properties

The dynamic viscosity measurements were carried out in an Anton Paar FRS 1600 high-temperature rheometer using a graphite measuring system, that is, crucible and spindle of 30- and 27.6-mm diameter, respectively. Both flow curves in the shear rate range of 80 to 200 s⁻¹ and dynamic viscosity values at a shear rate of 100 s⁻¹ were recorded at 20 and 50 °C.

2.3. Determination of specific heat capacities

Differential scanning calorimetry (DSC) measurement was performed with a SENSYS 3D DSC calorimeter. Absolute enthalpy calibration was carried out through a Joule effect. The continuous DSC method was used for the determination of hematite and BFSL, and the sample weight was approximately 27 mg. Aluminum crucibles were utilized for the analysis, with an empty crucible serving as a reference sample. The measurements were performed in a dynamic atmosphere of synthetic air at a heating rate of 1 °C·min⁻¹. The measured heat capacity values are reported for a temperature of 50 °C.

2.4. Ultrasonic disintegration of BFSL samples

To obtain suspensions of 1, 3, and 5% by weight, an appropriate amount of leached blast furnace sludge (BFSL) was dispersed in 20 ml of deionized water (0.1 µS·cm⁻¹) and ultrasonicated for 5 minutes using Omni Sonic Ruptor 400 homogenizer (OMNI INTERNATIONAL, Kennesaw, GA, USA). After ultrasonication, the dispersion was cooled down to ambient temperature and 0.1 ml of the dispersion was transferred to a 10 ml volumetric flask and filled with distilled water.

2.5. XRF, AAS, XRD, SEM, EDX and DLS methods

The composition of the unleached and leached blast furnace sludge was assessed using a Spectro Xepos X-ray fluorescence (XRF) analyzer and an AA280 FS atomic absorption spectrophotometer. XRD (X-ray powder diffraction) was carried out by a Bruker-AXS D8 Advance diffractometer with CuK α filtered radiation, voltage 40 kV, current 40 mA, step by step mode of 0.014° 2 θ , total time 25 s per step and angular extent 5–80° 2 θ . The semiquantitative composition was determined by the Rietveld method together with the internal standard method (ZnO, 10%). A FEI Quantum-650 FEG electron microscope operating under the following conditions (voltage 15 kV, current 8–10 nA, beam diameter 5.5 mm, low vacuum) and equipped with EDAX Galaxy EDX analyzer was used for taking SEM images. For dynamic light scattering (DLS) measurements, a disposable 10x10mm plastic cell (DTS0012) was filled with the sample and particle size was measured with Malvern Zetasizer Ultra (Malvern Instruments Ltd., Worcestershire, UK) analyzer at a backscattering light angle of 173° using ZS Xplorer software. All measurements were recorded as an average of three measurements and were carried out at 25 °C.

3. RESULTS AND DISCUSSION

The rheological behavior was assessed by measuring flow curves at 20 and 50 °C of the analyzed fluids containing micro- and nanosized hematite particles and BFSL particles. **Figure 1** shows the viscosity values obtained in the shear rate range between 80 and 200 s⁻¹.

Table 3 Dynamic viscosity values (mPa·s) of the analyzed suspensions at a shear rate of 100 s⁻¹

	Microhematite		Nanohematite		BFSL	
	20 °C	50 °C	20 °C	50 °C	20 °C	50 °C
1 wt%	1.6	1.9	1.0	0.9	1.6	1.7
3 wt%	2.0	1.9	1.2	1.0	2.1	2.0
5 wt%	1.9	1.9	1.4	1.2	2.4	2.2

All samples exhibited Newtonian behavior and had viscosity values higher than those for the base liquid at 20 and 50 °C, i.e., 1.001 and 0.788 mPa·s, respectively, with the slightest difference in the case of the hematite nanofluid. A comparison of viscosities at a shear rate of 100 s⁻¹ is given in **Table 3**.

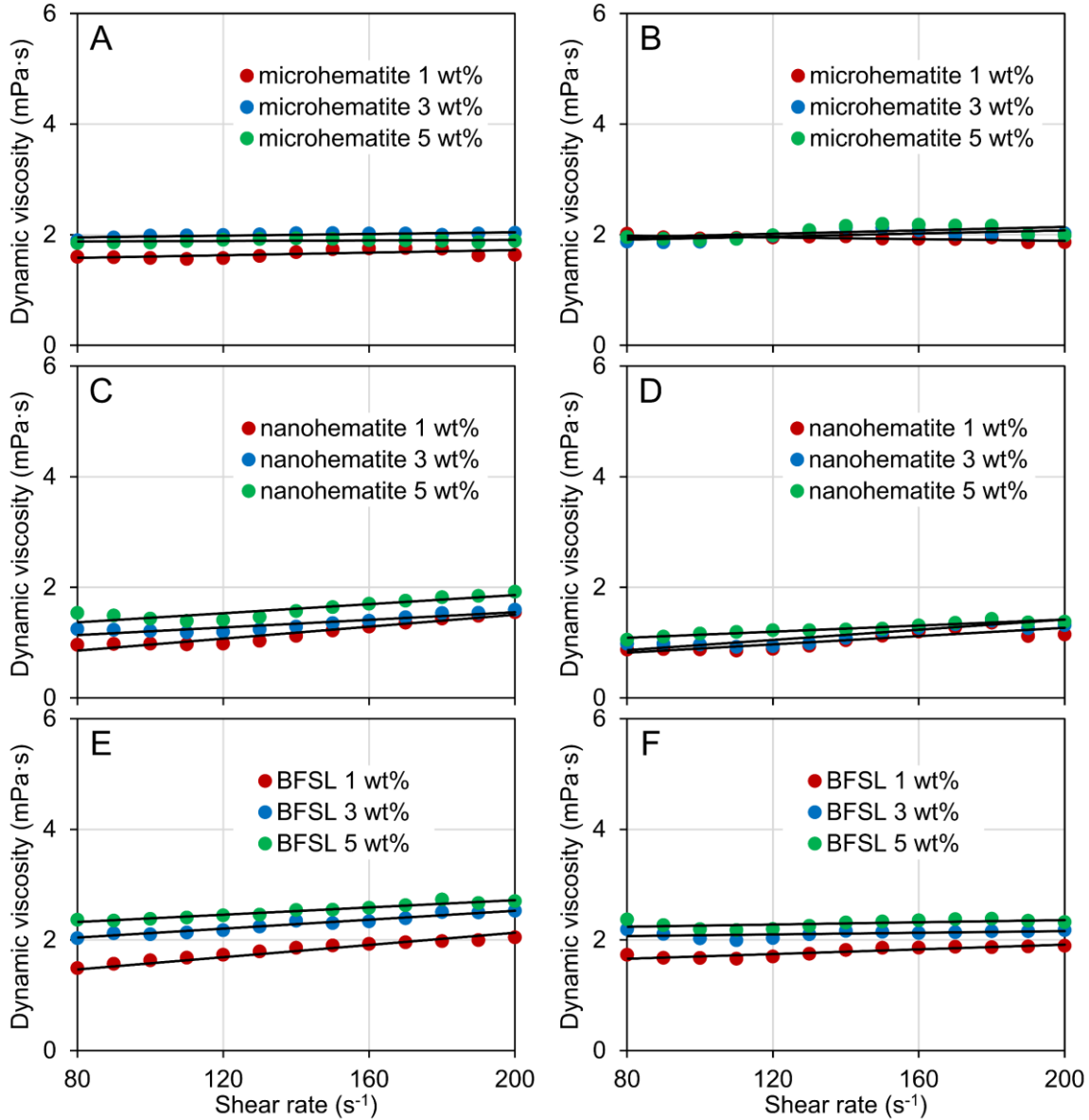


Figure 1 Flow curves for microhematite, nanohematite and BFSL suspensions at 20 °C (A, C, E) and 50 °C (B, D, F)

The specific heat capacity (SHC) of the BFSL particles was measured using a SENSYS calorimeter, while that for the nanoparticles was adopted and calculated according to [15]. The Brinkman model for concentrated solutions and suspensions was used to calculate volume concentrations (Equation (1)) [16], and the specific capacities of the nanofluids were obtained through the relationship proposed by Pak and Cho (Equation (2)) [17]. The calculated results are listed in **Table 4**, and the dynamic viscosity values were taken from **Table 3**.

$$\frac{\eta_{nf}}{\eta_{bf}} = (1 - \varphi_p)^{-\frac{5}{2}} \quad (1)$$

$$c_{p,nf} = (1 - \varphi_p)c_{p,bf} + \varphi_p c_{p,p} \quad (2)$$

where: η_{nf} is dynamic viscosity of nanofluid (mPa·s), η_{bf} is dynamic viscosity of base fluid (mPa·s), $c_{p,nf}$ is specific heat capacity of nanofluid ($J \cdot g^{-1} \cdot K^{-1}$), $c_{p,bf}$ is specific heat capacity of base fluid ($J \cdot g^{-1} \cdot K^{-1}$), $c_{p,p}$ is specific heat capacity of particles ($J \cdot g^{-1} \cdot K^{-1}$) and φ_p is volumetric concentration of particles.

Table 4 Calculated specific heat capacities of BFSL and nanohematite fluids for 50 °C

	nanohematite		BFSL	
	φ_p	$c_{p,nf}$ ($J \cdot g^{-1} \cdot K^{-1}$)	φ_p	$c_{p,nf}$ ($J \cdot g^{-1} \cdot K^{-1}$)
1 wt%	0.041	4.039	0.260	3.271
3 wt%	0.078	3.913	0.315	3.078
5 wt%	0.144	3.685	0.336	3.004

$$c_{p,p(BFSL)} = 0.676 J \cdot g^{-1} \cdot K^{-1}, c_{p,p(nanohematite)} = 0.739 J \cdot g^{-1} \cdot K^{-1}, c_{p,bf} = 4.181 J \cdot g^{-1} \cdot K^{-1}$$

Compared to the SHC of the base fluid, the SHC of the fluid containing nanohematite and BFSL decreased by 3-12% and 22-28%, respectively. In addition, the BFSL particles remained suspended in water for more than one week after ultrasonication and were therefore subjected to DLS and SEM/EDX analyses to elucidate the effect of ultrasonic treatment.

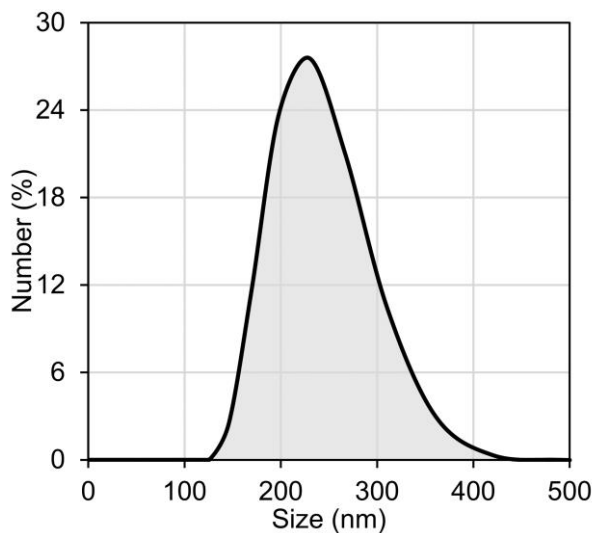


Figure 2 Size distribution of leached blast furnace sludge particles

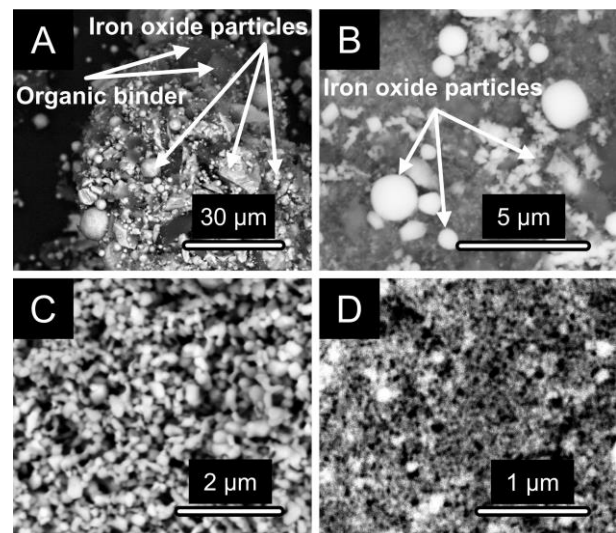


Figure 3 SEM analysis of BFSL (before A and after B sonication), microhematite (C) and nanohematite (D) particles

Figure 2 shows that BFSL is a dispersed system containing particles of sizes between 126 and 485 nm, with the main particle fraction having a size of 170 - 310 nm. SEM/EDX analysis showed that ultrasound disrupted organically bound aggregates into finer iron oxide particles (**Figure 3**).

4. CONCLUSION

This study set out to investigate the use of blast furnace sludge as a water-based heat transfer fluid in terms of assessing the dynamic viscosity and specific heat capacity values. For this purpose, it was acid leached to reduce the content of most elements except iron oxides, of which hematite was the most abundant. Using available analytical methods, the aqueous suspension of BFSL was analyzed and compared with model systems containing nano- and microhematite particles. It was found that the BFSL suspension exhibited relatively good stability and can be potentially used as a heat transfer fluid; however, it should be emphasized that significant further steps need to be taken in this area.

ACKNOWLEDGEMENTS

This work was supported by the project No.CZ.02.1.01/0.0/0.0/17_049/0008399 - EU and CR financial funds - provided by the Operational Programme Research, Development and Education, Call 02_17_049 Long-Term Intersectoral Cooperation for ITI, Managing Authority: Czech Republic - Ministry of Education, Youth and Sports, and student projects SP2022/68 and SP2022/39.

REFERENCES

- [1] CHOI, STEPHEN U.S., EASTMAN, JEFFREY A. Enhancing thermal conductivity of fluids with nanoparticles. In: *ASME International Mechanical Engineering Congress and Exposition*. San Francisco: ASME, 1995, pp. 99-105.
- [2] MURSHED, S.M.S., LEONG, K.C., YANG, C. Thermophysical and electrokinetic properties of nanofluids - A critical review. *Applied Thermal Engineering*. 2008, vol. 28, no. 17-18, pp. 2109-2125.
- [3] MEYER, J.P., ADIO, S.A., SHARIFPUR, M., NWOSU, P.N. The Viscosity of Nanofluids: A Review of the Theoretical, Empirical, and Numerical Models. *Heat Transfer Engineering*. 2016, vol. 37, no. 5, pp. 387-421.
- [4] HONG, T.-K., YANG, H.-S., CHOI, C.J. Study of the enhanced thermal conductivity of Fe nanofluids. *Journal of Applied Physics*. 2005, vol. 97, no. 6, art. no. 064311.
- [5] MAHBUBUL, I.M., SAIDUR, R., AMALINA, M.A. Investigation of viscosity of R123-TiO₂ nanorefrigerant. *International Journal of Mechanical and Materials Engineering*. 2012, vol. 7, no. 2, pp. 146 - 151.
- [6] MAHBUBUL, I.M., SAIDUR, R., AMALINA, M.A. Latest developments on the viscosity of nanofluids. *International Journal of Heat and Mass Transfer*. 2012, vol. 55, no. 4, pp. 874-885.
- [7] VAJJHA, R.S., DAS, D.K. A review and analysis on influence of temperature and concentration of nanofluids on thermophysical properties, heat transfer and pumping power. *International Journal of Heat and Mass Transfer*. 2012, vol. 55, no. 15-16, pp. 4063-4078.
- [8] SUNDAR, L.S., SHARMA, K.V., NAIK, M.T., SINGH, M.K. Empirical and theoretical correlations on viscosity of nanofluids: A review. *Renewable and Sustainable Energy Reviews*. 2013, vol. 25, pp. 670-686.
- [9] ALADE, I.O., ABD RAHMAN, M.A., ABBAS, Z., YAAKOB, Y., SALEH, T.A. Application of support vector regression and artificial neural network for prediction of specific heat capacity of aqueous nanofluids of copper oxide. *Solar Energy*. 2020, vol. 197, pp. 485-490.
- [10] SHAHRUL, I.M., MAHBUBUL, I.M., KHALEDUZZAMAN, S.S., SAIDUR, R., SABRI, M.F.M. A comparative review on the specific heat of nanofluids for energy perspective. *Renewable and Sustainable Energy Reviews*. 2014, vol. 38, pp. 88-98.
- [11] ELSAIDY, A., VALLEJO, J.P., SALGUEIRIÑO, V., LUGO, L. Tuning the thermal properties of aqueous nanofluids by taking advantage of size-customized clusters of iron oxide nanoparticles. *Journal of Molecular Liquids*. 2021, vol. 344, art. no. 117727.
- [12] SONAWANE, S.S., JUWAR, V. Optimization of conditions for an enhancement of thermal conductivity and minimization of viscosity of ethylene glycol based Fe₃O₄ nanofluid. *Applied Thermal Engineering*. 2016, vol. 109, pp. 121-129.
- [13] HATAMI, M., MOHAMMADI-REZAEI, S., TAHARI, M., JING, D. Recent developments in magneto-hydrodynamic Fe₃O₄ nanofluids for different molecular applications: A review study. *Journal of Molecular Liquids*. 2018, vol. 250, pp. 244-258.
- [14] KARIMI, A., GOHARKHAH, M., ASHJAEI, M., SHAFII, M.B. Thermal Conductivity of Fe₂O₃ and Fe₃O₄ Magnetic Nanofluids Under the Influence of Magnetic Field. *International Journal of Thermophysics*. 2015, vol. 36, no. 10-11, pp. 2720-2739.
- [15] SNOW, C.L., LEE, C.R., SHI, Q., BOERIO-GOATES, J., WOODFIELD, B.F. Size-dependence of the heat capacity and thermodynamic properties of hematite (α -Fe₂O₃). *Journal of Chemical Thermodynamics*. 2010, vol. 42, no. 9, pp. 1142-1151.
- [16] BRINKMAN, H.C. The viscosity of concentrated suspensions and solutions. *The Journal of Chemical Physics*. 1952, vol. 20, no. 4, pp. 571.
- [17] PAK, B.C., CHO, Y.I. Hydrodynamic and heat transfer study of dispersed fluids with submicron metallic oxide particles. *Experimental Heat Transfer*. 1998, vol. 11, no. 2, pp. 151-170.